Effects of Rhubarb on Intestinal Flora and Toll-Like Receptors of Intestinal Mucosa in Rats With Severe Acute Pancreatitis

Ping Yao, MD, Min Cui, MD,† Yan Li, MD,† Yiyun Deng, MD, PhD,‡ and Hao Wu, MD, PhD§*

Objective: The aim of this study was to examine the effects of rhubarb on intestinal flora and toll-like receptors (TLRs) of intestinal mucosa in rats with severe acute pancreatitis (SAP).

Methods: Healthy male Sprague-Dawley rats were randomly allocated into sham-operated surgical model of SAP without or with postoperative rhubarb treatment groups (7 in each group). Rats in with rhubarb group received 10% rhubarb decoction (1 mL/200 g) through tube feeding at every 8 hours during postoperative 24 hours. Serum amylase, amount of intestinal flora, and TLR2/TLR4 messenger RNA expression in intestinal mucosa were tested among 3 groups at postoperative 24 hours.

Results: TLR2 and TLR4 messenger RNA expression levels in intestinal mucosa in SAP without rhubarb group were significantly higher than those in sham-operated or SAP with rhubarb groups ($P < 0.05$). The amount of intestinal lactobacilli and bifidobacteria in SAP without rhubarb group were significantly fewer than in those sham-operated group ($P < 0.05$) but not significantly different from those in SAP with rhubarb group ($P > 0.05$). The amount of intestinal *Escherichia coli* was relatively higher in SAP group than in sham-operated group ($P > 0.05$) but lesser in rhubarb treatment group ($P > 0.05$).

Conclusions: Rhubarb might maintain the intestinal mucosal barrier through regulating intestinal flora and inhibiting intestinal inflammatory response in rats with SAP.

Key Words: rhubarb, toll-like receptors, lactobacilli, bifidobacterium, *Escherichia coli*, intestinal mucosal barrier

(*Pancreas* 2015;44: 799–804)

Severe acute pancreatitis (SAP) is a critical illness associated with long-term treatment and high mortality (up to 15%–30%). Organ failure is an important determinant of the mortality in SAP. Under normal circumstances, organ failure mainly occurs in 3 to 4 weeks after the onset of SAP, and approximately 30% of the patients experience necrotizing pancreatitis and secondary pancreatic infection. Owing to the progress of SAP treatment, the cure rate of SAP has relatively been increased in recent years; the overall mortality of SAP, however, remains up to approximately 17%.[1,2]

Severe acute pancreatitis is often complicated by intestinal mucosal barrier dysfunction,[3,4] which is a major factor that promotes SAP deterioration and affects the prognosis.[5–7] The intestine system provides the largest reservoir of bacteria and endotoxins in the human body. Under normal circumstances, the intestinal mucosal barrier possesses complete function with no harm to human body. However, the intestinal mucosal barrier dysfunction can lead to the translocation of intestinal flora and endotoxin with secondary intestinal infection in SAP. Deaths caused by infection-related complications account for 80% of total deaths caused by SAP.[8]

Toll-like receptors (TLRs) are important transmembrane and signal transduction receptors in congenital immunity, which have a key role in the intestinal mucosal immune barrier. Toll-like receptors can activate the production of a series of inflammatory and anti-inflammatory cytokines and chemokines, which are involved in the regulation of different intestinal inflammatory responses. Chinese rhubarb (*Rheum palmatum* L.) is a stimulant laxative.[9] For instance, rhubarb can reduce the level of serum amylase (AMY), tumor necrosis factor α (TNF-α), interleukin (IL) 6,[10] IL-8, IL-1β,[11] and MCP-1[12] in rats with SAP; rhubarb can reduce the intestinal permeability,[10] bacteria translocation,[13] and promote intestinal peristalsis[14] in rats with SAP. However, previous studies have only examined gastrointestinal pathomorphology and surface structure indicators after rhubarb treatment of gastrointestinal mucosa.

To date, no in-depth study has explored the mechanisms through which rhubarb affects gastrointestinal mucosa regarding physiological function and immunoregulation; meanwhile, the work rhubarb on the intestinal microbiota has not been involved in the study of the past. In the present study, the effects of rhubarb on the number of intestinal flora and level of TLRs messenger RNA (mRNA) expression in SAP were examined to explore the mechanisms through which rhubarb protects the intestinal mucosal barrier in SAP.

MATERIALS AND METHODS

Reagents and Instruments

Reagents and assay kits used in this study mainly included sodium taurocholate (Sigma Chemical Co, St Louis, Mo), 10% rhubarb decoction (prepared by the Department of Pharmaceutical Preparation, Xinjiang Medical University), TRIzol Reagent (Invitrogen, Carlsbad, Calif), RevertAid first strand complementary DNA (cDNA) synthesis kit (Thermo Fisher Scientific Inc, Waltham, Mass), agarose gel DNA extraction kit (centrifugal columnar; Tiangen, Beijing, China), primers (designed by BioMed, Beijing, China), SYBR Green polymerase chain reaction (PCR) kit (Qiagen, Hilden, Germany), QIAamp DNA stool mini kit (Qiagen), bacterial genomic DNA extraction kit (BioMed), and 2× Taq PCR master mix (BioMed).

Instruments used in this study mainly included −80°C ultra–low temperature freezer, gradient PCR thermal cycler (C1000 Thermal Cycler; Bio-Rad Laboratories, Hercules, Calif), quantitative real-time PCR machine (iCycler iQ5; Bio-Rad Laboratories), and gel electrophoresis and image analysis system.

Animal and Groups

Twenty-one sanitary-grade healthy male Sprague-Dawley rats (body weight, 220–300 g) were provided by the Experimental Animal Center of Xinjiang Medical University, and the study was

From the Departments of *Gastroenterology and †Gastroenterology, the First Affiliated Hospital of Xinjiang Medical University, Urumqi, Xinjiang Uygur Autonomous Region; and ‡Intensive Care Unit and §Department of Gastroenterology, West China Hospital, Sichuan University, Chengdu, Sichuan Province, China.

Received for publication February 27, 2014; accepted October 29, 2014.

Reprints: Hao Wu, MD, PhD, Department of Gastroenterology, West China Hospital, Sichuan University, 37 Guo Xue Xiang, Chengdu 610041, Sichuan Province, PR China (e-mail: wuhao19710511@sina.com).

This study was supported by the Xinjiang Uygur Autonomous Region Natural Science Foundation (number 201233146-15).

The authors declare no conflict of interest.

approved by the animal ethics committee of the First Affiliated Hospital of Xinjiang Medical University (approval number, IACUC-20121127007; animal license number, SYXK[Xinjiang] 2010-0003). The animals were randomly divided into the sham-operated group (S), SAP group (P), and rhubarb treatment group (T) (n = 7 each).

Animal Model and Surgical Techniques

Before surgery, all groups of animals were fasted for 12 hours with free access to water and then anesthetized through intraperitoneal injection of ketamine solution. Upon satisfactory anesthesia, the animal was fixed on an operating table for skin preparation of the abdominal surgical area, followed by routine disinfection and draping.

Group S

An incision was made right in the middle of the upper abdomen of the rats. The duodenum was exposed, lifted, and pulled. Only after a flip, the duodenum was set back, and the abdomen was closed by 2 layers.

Group P

An incision was made right in the middle of the upper abdomen of rats. The duodenum was exposed, lifted, and pulled. After the pancreaticobiliary and hilar bile ducts were identified, the latter was temporarily occluded with a small artery clamp at the fossae transversalis hepatis side of the ligamentum hepatoduodenale. The opening of duodenal papilla was checked along the pancreaticobiliary duct, and an avascular area was selected from the duodenal wall slightly below the opening of papilla. The duodenal wall was pierced with a needle of number 4.5 scalp acupuncture at a 10- to 15-degree angle to the plane of the intestine and pancreas. The needle pierced through the papilla into the pancreaticobiliary duct and was then fixed. The open ends of pancreaticobiliary duct and duodenum were temporarily blocked with a cotton swab, and 5% taurocholate sodium (1 mL/kg) was injected into the pancreaticobiliary duct at a fixed rate of 0.2 mL/min.[15] After the injection, the needle was pulled out, and the needle hole was pressed with a cotton swab for 2 minutes. Then, the artery clamp was removed from the pancreaticobiliary duct. It was made sure that no hemorrhage and bile leakage occurred, and occurrence of congestion and edema in the pancreas was examined. Finally, the intestine duct was set back, and the abdomen was closed by 2 layers.

Group T

After the successful establishment of SAP rat model, animals were intragastrically administered with 10% rhubarb decoction (1 mL/200 g) immediately at every 8 hours till 24 hours postsurgery.

After surgery, animals of all groups received subcutaneous (normal saline, 2 mL/100 g) at every 6 hours till 24 hours postsurgery. After waking up, animals were fasted with free access to water and kept in separate cages.

Postoperative Examinations

At 24 hours postoperative, AMY was measured in arterial blood. Terminal ileum and pancreatic tissue specimens were fixed in 4% paraformaldehyde followed by hematoxylin and eosin (HE) staining and histopathological scoring. A proportion of terminal ileum tissue specimens was preserved at −80°C before real-time quantitative PCR assay of TLR4 and TLR2 mRNA expression levels in intestinal mucosa. Stool specimens from the ileocecus were frozen at −80°C and then used for quantitative assay of intestinal flora.

Serology

Serum AMY was measured using a Mindray BS-120 automatic biochemistry analyzer (Shenzhen, China).

Histology

Terminal ileum and pancreatic tissue specimens, which were fixed in 4% paraformaldehyde, were dehydrated, embedded, and sectioned after routine procedure. After HE staining, tissue sections were examined by microscopy. Per the modified evaluation criteria of Schmidt,[16] 5 fields of view were examined, and the mean score was taken to reflect pathological changes in the pancreas. Ileum tissue injury was scored as per the method of Chiu et al,[17] and the mean score of 5 fields of view was taken to reflect pathological changes in the terminal ileum.

Gel Electrophoresis

The specificity of TLR PCR amplification and size consistency of PCR products with DNA fragments expected in primer design and synthesis were determined by running 2% agarose gel electrophoresis of the TLR4 and TLR2 PCR products. The size of target gene fragments was measured with a 50 base pair (bp) DNA Ladder (Tiangen).

Real-Time Quantitative PCR

Real-Time Quantitative PCR Assay of TLR2 and TLR4 mRNA Levels in Terminal Ileum

Total RNA was extracted from terminal ileum tissue specimens using TRIzol Reagent (Invitrogen; Carlsbad, Calif). The purity of RNA extract was tested by spectrophotometry analysis of optical density (OD, OD_{260}/OD_{280} = 1.95–2.0). The total RNA (1 μg each) was used as template for cDNA synthesis through reverse transcription with oligo (dT) primers. The obtained cDNA (2 μL each) was used as a template for PCR amplification with ACTB (β-Actin) as an internal reference. The PCR products (2 μL each) were electrophoresed on 2% agarose gel, photographed, and purified from the gel. The relative levels of TLR2 and TLR4 mRNA expression were determined using a standard curve method, and the results were expressed as the ratio of target genes (*TLR2*, *TLR4*) to internal reference (ACTB (β-Actin)). Primer sequences and PCR conditions are shown in Table 1.

Real-Time Quantitative PCR Assay of Intestinal Lactobacilli, Bifidobacterium, and *Escherichia coli* in Ileocecus

Bacterial genomic DNA was extracted from stool specimens using a QIAamp DNA stool mini kit per manufacturer's instructions. Purity of DNA extract was tested by spectrophotometry analysis of OD value (OD_{260}/OD_{280} = 1.7–1.9). Specific PCR primers were designed for *E. coli*, Lactobacilli, bifidobacterium, and internal reference per the literature[18–20] (Table 2). Polymerase chain reaction amplification was conducted using cDNA (2 μL each) as the template with an internal reference. The PCR products (2 μL each) were checked by 2% agarose gel electrophoresis, photographed, and purified. The amplified DNA fragments were also compared with standard DNA of *E. coli*, Lactobacilli, and bifidobacterium. The relative levels of intestinal *E. coli*, Lactobacilli, and bifidobacterium gene expression were determined using a standard curve method. Results were expressed as the ratio of target genes (*E. coli*, Lactobacilli, and bifidobacterium) to internal reference. Primer sequences and PCR conditions are shown in Table 2.

TABLE 1. Primer Sequences and PCR Conditions

Target Gene	Primer Sequence (5′ → 3′)	Temperature	Product Length, bp
TLR2	F: 5′-CGCTTCCTGAACTTGTCC-3′ R: 5′-GGTTGTCACCTGCTTCCA-3′	59.6°C	285
TLR4	F: 5′-GCATCATCTTCATTGTCCTTGAGA-3′ R: 5′-CTCCCACTCGAGGTAGGTGTTT-3′	61.5°C	100
ACTB (β-Actin)	F: 5′-ACTGCCCTGGCTCCTAGCA-3′ R: 5′-GCCAGGATAGAGCCACCAATC-3′	54.7°C	85

Statistical Analyses

All experimental data were processed in SPSS 17.0 statistical package (SPSS Inc, Chicago, Ill). Data were expressed as mean (SD) and subjected to tests for homogeneity of variance and normality ($P > 0.05$ for both). Intergroup comparisons were performed using 1-way analysis of variance, and significant difference among means was identified by Fisher least significant difference test at the level of $\alpha = 0.05$. A 2-sided P value less than 0.05 was considered statistically significant.

RESULTS

Histopathological Changes in Pancreas and Ileum

General Histopathological Changes

At 24 hours postsurgery, animals of group S had no obvious abnormalities in the pancreas and ileum (Figs. 1A, D). Animals of group P had massive exudative hemorrhagic or yellow ascites in the abdominal cavity; significant swelling, hardening, and visible necrosis of the pancreas in a gray brown color; large amounts of peripancreatic saponification spots; and thickening of the ileum due to edema (Figs. 1B, E). By comparison, animals of group T had a little exudative yellow ascites in the abdominal cavity; light swelling, hemorrhage, and necrosis in the pancreas; few saponification spots; and swelling of the ileum to a lesser degree (Figs. 1C, F).

Histopathological Changes in the Pancreas

Under light microscope, animals of group S had a clear structure of pancreatic lobules with a lack of abnormal changes (Fig. 2A). Animals of group P had diffused interlobular septal thickening, punctate intercellular septal thickening, and splinter hemorrhage in the pancreas, with massive acinar necrosis and inflammation cell infiltration (Fig. 2B). Animals of group T had minor inflammatory cell infiltration in the pancreas, with spotty necrosis observed occasionally (Fig. 2C).

Histopathological Changes in the Ileum

Under light microscope, animals of group S had an intact structure of villi in the ileum without stromal edema or inflammatory cell infiltration (Fig. 2D). Animals of group P had severe intestinal mucosal edema; mucosal epithelial cell degradation and necrosis; exfoliation, fusion, and shortening of villi; intraluminal exfoliation of necrotic tissues; massive inflammatory cell infiltration in the lamina propria; and vasodilation in submucosal arterioles (Fig. 2E). Compared with group P, animals of group T had intestinal mucosal edema to a lesser degree, generally intact epithelial cells, occasional vasodilation, little inflammatory cell infiltration in the lamina propria, and enlarged and increased goblet cells (Fig. 2F).

Intergroup Comparison of Serum AMY, Pancreatic and Intestinal Injury Scores, and TLR mRNA Expression Levels

Serum AMY and Pancreatic Injury Scoring

Serum AMY and pancreatic injury score of animals were both higher in groups P and T than in group S ($P < 0.05$ for both comparisons) and significantly higher in group P than in group T ($P < 0.05$, Table 3). This result indicated that the establishment of SAP model was successful.

Intestinal Injury Scoring

Intestinal injury score was significantly higher in groups P and T than in group S ($P < 0.05$ for both comparisons) and significantly higher in group P than in group T ($P < 0.05$, Table 3).

TLR mRNA Expression Levels in Intestinal Mucosa

TLR2 and TLR4 mRNA expression levels were both higher in group P than in groups S and T, showing statistically significant differences ($P < 0.05$ for both comparisons). TLR2 and TLR4 mRNA expression levels were slightly higher in group T than in group S, showing no statistically significant differences ($P > 0.05$).

TABLE 2. Primer Sequences and PCR Conditions

Bacteria	Target Gene	Primer Sequence (5′ → 3′)	Temperature	Product Length, bp
E. coli	16S rDNA	F: 5′-GTTAATACCTTTGCTCATTGA-3′ R: 5′-ACCAGGGTATCTTAATCCTGTT-3′	49.1°C	340
Lactobacilli	16S rDNA	F: 5′-AGCAGTAGGGAATCTTCCA-3′ R: 5′-CACCGCTACACATGGAG-3′	54.5°C	341
Bifidobacterium	16S rDNA	F: 5′-TCGCGTC(C/T) GGTGTGAAAG-3′ R: 5′-CCACATCCAGC(A/G) TCCAC-3′	62°C	243
Internal reference	16S rDNA	F:5′-ACGGGGGGCCTACGGGAGGCAGCAG-3′ R:5′-ATTACCGCGGCTGCTGG-3′	65°C	357

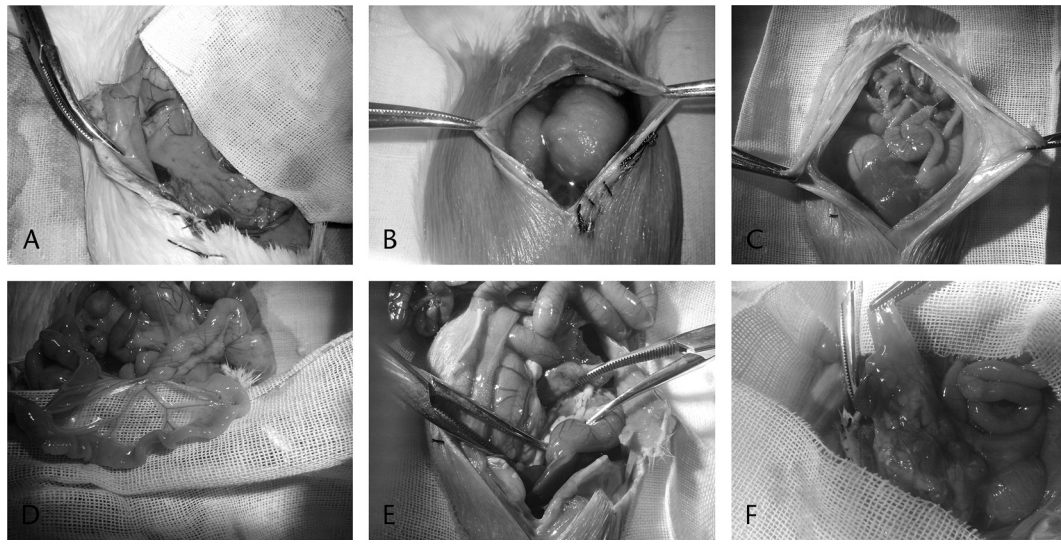

FIGURE 1. A, Group S: pancreatic tissue. B, Group P: massive ascites (wet cotton swab). C, Group T: ileum with little ascites. D, Group S: ileum tissue. E, Group P: ileum and pancreas. F, Group T: pancreatic tissue.

DNA Bands of TLR PCR Products in Gel Electrophoresis

The PCR products of TLR2 and TLR4 both showed a single specific DNA band in electrophoretic gel image (285 and 100 bp, respectively; Fig. 3). These 2 sizes of PCR products were consistent with the lengths of DNA fragments expected in primer design and synthesis (Table 1). Both PCR products displayed brighter DNA bands in gel electrophoresis, with the brightness clearly higher in groups P than in groups S and T, and higher in group T than in group S. These results confirmed that TLR2 and TLR4 expression levels were higher in group P than in group S and lower in group T than in group P.

Intergroup Comparison of Intestinal Flora in Cecal Contents

Compared with those of group S, animals of group P had increased number of *E. coli* but reduced number of *Bifidobacterium* and Lactobacilli in cecal contents, showing statistically significant differences ($P < 0.05$ for all comparisons, Table 4). At 24 hours after rhubarb treatment, the number of *E. coli* relatively declined, whereas those of *Bifidobacterium* and Lactobacilli slightly increased in cecal contents, with no statistically significant differences for any comparisons ($P > 0.05$, Table 4).

DISCUSSION

Intestinal mucosal barrier comprises the mechanical barrier, immune barrier, and biochemical and microbial barrier, which plays a decisive role in the pathogenesis and development of SAP.[21] Early SAP is associated with intestinal immune barrier dysfunction,[22] gastrointestinal microbial imbalance,[23] and mucosal barrier functional changes. The above changes can lead to pancreatic necrosis and cause intestinal bacterial translocation, increasing the incidence of complications such as pancreatic necrosis and organ failure.

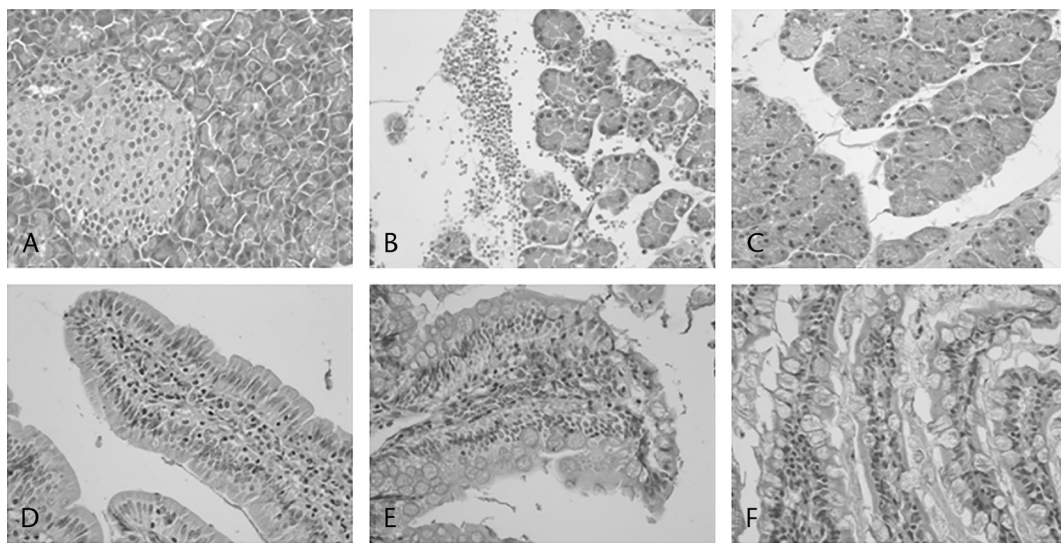

FIGURE 2. A, Group S: pancreatic tissue (HE ×400). B, Group P: pancreatic tissue (HE ×400). C, Group T: pancreatic tissue (HE ×400). D, Group S: ileum tissue (HE ×400). E, Group P: ileum tissue (HE ×400). F, Group T: ileum tissue (HE ×400).

TABLE 3. AMY, Pancreatic and Intestinal Injury Scores, and TLR mRNA Expression Levels (Mean [SD], n = 7) in Experimental Rats

Rat Group	AMY, μ/L	Pancreatic Injury Scores	Intestinal Injury Scores	TLR2 mRNA Expression Level	TLR4 mRNA Expression Level
Sham operated	2425.73 (239.60)*	0.76 (0.21)*	1.21 (0.49)*	0.017 (0.008)*	0.27 (0.10)*
SAP	8172.40 (1315.30)†	6.89 (0.48)†	4.46 (0.37)†	0.037 (0.017)†	0.73 (0.14)†
Rhubarb treatment	5849.47 (1410.79)*†	4.94 (0.53)*†	3.25 (0.25)*†	0.022 (0.005)*	0.32 (0.17)*

*Comparison with the SAP group ($P < 0.05$).

†Comparison with the sham-operated group ($P < 0.05$).

Toll-like receptors serve as important transmembrane and signal transduction receptors for innate immunity, playing a key role in intestinal mucosal immune barrier. TLR2 ligand is the lipoteichoic acid of Gram-positive bacteria, and TLR4 ligand is the lipopolysaccharide of Gram-negative bacteria.[24] Once the pathogen-associated molecular patterns are identified, TLRs transmit signals into the cytoplasm through the translation initiation region, eventually activating nuclear factor-κ-gene binding and MAPK (mitogen-activated protein kinase) P38 through MYD88, IL-1 receptor-associated kinase, and TNF receptor–associated factor 6. In this way, a variety of cytokines including IL-6, IL-1, IL-8, IL-10, IL-12, TNF-α, nitric oxide synthase, and B7 molecules leads to inflammatory response.[25,26]

In the present study, the results showed that compared with animals of the sham-operated group, SAP rats experienced severer damage to pancreatic and terminal ileum tissues (Figs. 1, 2; Table 3), with less numbers of intestinal lactobacilli and bifidobacteria but a more number of *E. coli* (Table 4), which was consistent with the previous finding by Quigley and Quera.[27] Severe acute pancreatitis rats had relatively high TLR2 and TLR4 mRNA expression levels (Table 3). It could be considered that in the case of SAP, intestinal dysfunction of blood supply could lead to the shortening of intestinal mucosal villi, exfoliation and functional decline of goblet cells, and reduction of mucous secretions including sIgA in the intestinal lumen.[28] In addition, quantitative decreases in the numbers of intestinal lactobacilli and bifidobacteria could reduce the original colonization resistance of probiotic bacteria.[29,30] Correspondingly, the number of opportunistic bacterial pathogens increases, and their metabolites (bacterial protease) cause damage to microvillus membrane proteins of intestinal epithelial cells and villus tissue, leading to intestinal mucosal barrier dysfunction.[31,32] Highly up-regulated levels of TLR2 and TLR4 mRNA expression in intestinal mucosa cause excessive activation of nuclear factor-κ-gene binding and trigger intestinal inflammation, once again increasing the severity of damage of intestinal mucosal barrier. The damage of intestinal mucosal barrier reduces the number of colonized probiotic bacteria and thus promotes bacterial translocation, further damaging the intestinal microbial barrier[33] and inducing the subsequent systemic inflammatory response syndrome and multiple organ dysfunction syndrome. Thus, sepsis, infection and necrosis, organ failure, and even death are closely related to the intestinal mucosal barrier function in SAP.[5]

After the treatment of SAP with rhubarb, TLR2 and TLR4 mRNA expression levels both declined, with increasing tendencies in the number of intestinal Lactobacilli and Bifidobacterium and a declining tendency in the number of *E. coli* (Table 3). In addition, it was observed that the injuries of the pancreas and ileum in rats were significantly mitigated in the rhubarb treatment group than in the SAP group. Rhubarb induces intestinal epithelial hyperplasia and forms artificial inflammation of the intestinal mucosa. Such artificial inflammation accelerates epithelial cell renewal with compositional changes, thus rapidly changing physiological functions of the intestinal tract; that is, intestinal mucosa is transformed from absorption-based epithelia to immune secretion-based epithelia. The results of HE staining showed that goblet cells were increased quantitatively and enlarged morphologically in the ileum of SAP rats receiving rhubarb treatment. This observation demonstrates that rhubarb accelerates epithelial cell renewal and increases the secretory cells. The increased numbers of intestinal probiotics such as Lactobacilli and Bifidobacterium enhance their original colonization resistance, whereas the down-regulated TLR2 and TLR4 mRNA expression inhibits the occurrence and development of inflammatory responses. Joint action of multiple protective factors contributes to the recovery of the mechanical, microbial, immune, and biochemical barriers. Recent studies have shown that rhubarb also has multiple effects for enhancement of peristalsis, inhibition of inflammatory cytokines, removal of intestinal toxins and bacteria, prevention of bacterial translocation, improvement of intestinal

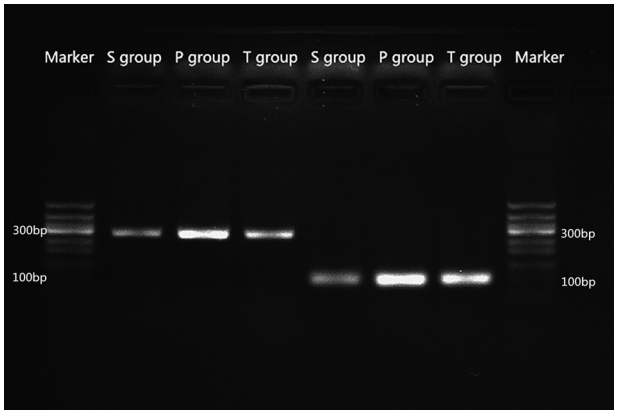

FIGURE 3. Electrophoretic gel image of TLR2 and TLR4 PCR products.

TABLE 4. Expression Levels of Intestinal Bacteria in Rat Cecum (Mean [SD], n = 7)

Rat Group	*E. coli* ($\times 10^{-5}$)	Bifidobacterium ($\times 10^{-3}$)	Lactobacilli ($\times 10^{-5}$)
Sham operated	4.16 (2.58)	22.07 (15.09)	24.42 (9.90)
SAP	19.43 (7.16)*	1.33 (0.67)*	9.17 (6.83)*
Rhubarb treatment	15.93 (15.21)*	2.29 (1.37)*	11.15 (4.66)*

*Comparison with the sham-operated group ($P < 0.05$).

and pancreatic microcirculation, cholagogue, inhibition of pancreatic secretion, antioxidation, reduction of capillary vascular permeability, promotion of blood circulation, and hemostasis.[11,34–37] All these effects are beneficial to reduce the incidences of subsequent systemic inflammatory response syndrome and multiple organ dysfunction syndrome in SAP.

This study has demonstrated that in the treatment of rats with SAP, rhubarb effectively repairs the intestinal mucosal barrier, regulates intestinal flora, inhibits intestinal inflammation, and reduces severe complications of SAP, ultimately improving the prognosis and outcome of the disease. However, the exact immune molecular regulation mechanisms of rhubarb on intestinal flora and intestinal mucosal barrier need to be studied further.

REFERENCES

1. Servin-Torres E, Velázquez-Garcia JA, Delgadillo-Teyer G, et al. Severe acute pancreatitis: surgical management in a third-level hospital [in Spanish]. *Cir Cir*. 2009;77:407–410.
2. Banks PA, Freeman MLPractice Parameters Committee of the American College of Gastroenterology. Practice guidelines in acute pancreatitis. *Am J Gastroenterol*. 2006;101:2379–2400.
3. Rychter JW, van Minnen LP, Verheem A, et al. Pretreatment but not treatment with probiotics abolishes mouse intestinal barrier dysfunction in acute pancreatitis. *Surgery*. 2009;145:157–167.
4. Besselink MG, van Santvoort HC, Renooij W, et al. Intestinal barrier dysfunction in a randomized trial of a specific probiotic composition in acute pancreatitis. *Ann Surg*. 2009;250:712–719.
5. Liu H, Li W, Wang X, et al. Early gut mucosal dysfunction in patients with acute pancreatitis. *Pancreas*. 2008;36:192–196.
6. Assimakopoulos SF, Vagianos CE, Patsoukis N, et al. Evidence for intestinal oxidative stress in obstructive jaundice-induced gut barrier dysfunction in rats. *Acta Physiol Scand*. 2004;180:177–185.
7. Pearce CB, Zinkevich V, Beech I, et al. Using the polymerase chain reaction coupled with denaturing gradient gel electrophoresis to investigate the association between bacterial translocation and systemic inflammatory response syndrome in predicted acute severe pancreatitis. *World J Gastroenterol*. 2005;11:7142–7147.
8. Dambrauskas Z, Gulbinas A, Pundzius J, et al. Meta-analysis of prophylactic parenteral antibiotic use in acute necrotizing pancreatitis. *Medicina (Kaunas)*. 2007;43:291–300.
9. Wilson P, Manji M, Neoptolemos J. Acute pancreatitis as a model of sepsis. *J Antimicrob Chemother*. 1998;41:51–63.
10. Wu L, Liu X, Cai H, et al. Effects of Dahuang Decociton on the STAT3 expression in pancreatic tissue of rats with severe acute pancreatitis. *China J Tradit Chin Med Pharmacy*. 2012;27:933–936.
11. Wang L, Yu L, Wang Y, et al. The protection mechanism of emodin on intestinal mucosa barrier in rats with severe acute pancreatitis. *Chin J Gerontol*. 2012;32:2319–2321.
12. Feng Z, Zou X, Xu Z, et al. Effects of Dahuang on the expression of inflammatory factors in severe pancreatitis rats. *Chin J Integr Med Digestion*. 2007;15:380–381.
13. Shi C, Jiang L, Duan Z, et al. The effect of rhubarb on T-lymphocyte subset and intestinal bacterial translocation in rat with severe acute pancreatitis. *Guizhou Med J*. 2008;32:584–585.
14. Chen X, Ran R. Rhubarb decoction prevents intestinal bacterial translocation during necrotic pancreatitis [in Chinese]. *Hua Xi Yi Ke Da Xue Xue Bao*. 1996;27:418–421.
15. Goldenberg A, Romeo AC, Moreira MB, et al. Experimental model of severe acute pancreatitis in rabbits. *Acta Cir Bras*. 2007;22:366–371.
16. Surbatović M, Jovanović K, Radaković S, et al. Pathophysiological aspects of severe acute pancreatitis-associated lung injury [in Serbian]. *Srp Arh Celok Lek*. 2005;133:76–81.
17. Chiu CJ, McArdle AH, Brown R, et al. Intestinal mucosal lesion in low-flow states. I. A morphological, hemodynamic, and metabolic reappraisal. *Arch Surg*. 1970;101:478–483.
18. Song M-R, Yao P. Application of fluorescent real-time polymerase chain reaction in quantification of *Escherichia coli*, *Lactobacillus* and Bifidobacteria in ulcerative colitis patients. *Chin J Microecology*. 2012; 24:239–243.
19. Rinttilä T, Kassinen A, Malinen E, et al. Development of an extensive set of 16S rDNA-targeted primers for quantification of pathogenic and indigenous bacteria in faecal samples by real-time PCR. *J Appl Microbiol*. 2004;97:1166–1177.
20. Marchesi J, Shanahan F. The normal intestinal microbiota. *Curr Opin Infect Dis*. 2007;20:508–513.
21. Koh YY, Jeon WK, Cho YK, et al. The effect of intestinal permeability and endotoxemia on the prognosis of acute pancreatitis. *Gut Liver*. 2012;6: 505–511.
22. Li JP, Yang J, Huang JR, et al. Immunosuppression and the infection in patients with early SAP. *Front Biosci (Landmark Ed)*. 2013;18:892–900.
23. Fritz S, Hackert T, Hartwig W, et al. Bacterial translocation and infected pancreatic necrosis in acute necrotizing pancreatitis derives from small bowel rather than from colon. *Am J Surg*. 2010;200:111–117.
24. Albiger B, Dahlberg S, Henriques-Normark B, et al. Role of the innate immune system in host defence against bacterial infections: focus on the Toll-like receptors. *J Intern Med*. 2007;261:511–528.
25. Yamamoto M, Akira S. Mechanisms of innate immune responses mediated by Toll-like receptors. *Clin Appl Immunol Rev*. 2005;5:167–183.
26. Atreya I, Atreya R, Neurath MF. NF-kappaB in inflammatory bowel disease. *J Intern Med*. 2008;263:591–596.
27. Quigley EM, Quera R. Small intestinal bacterial overgrowth: roles of antibiotics, prebiotics, and probiotics. *Gastroenterology*. 2006;130: S78–S90.
28. Wang H, Li F, Jiabang S. The damage and prevention of intestinal mucosal barrier function in severe acute pancreatitis. *China Mod Gen Surg*. 2007;7:321–326.
29. Turroni F, van Sinderen D, Ventura M. Genomics and ecological overview of the genus *Bifidobacterium*. *Int J Food Microbiol*. 2011; 149:37–44.
30. Hörmannsperger G, Haller D. Molecular crosstalk of probiotic bacteria with the intestinal immune system: clinical relevance in the context of inflammatory bowel disease. *Int J Med Microbiol*. 2010;300:63–73.
31. Valladares R, Sankar D, Li N, et al. Lactobacillus johnsonii N6.2 mitigates the development of type 1 diabetes in BB-DP rats. *PLoS One*. 2010; 5:e10507.
32. Sansonetti PJ, Medzhitov R. Learning tolerance while fighting ignorance. *Cell*. 2009;138:416–420.
33. Liu ZH, Peng JS, Li CJ, et al. A simple taurocholate-induced model of severe acute pancreatitis in rats. *World J Gastroenterol*. 2009;15: 5732–5739.
34. Qi W, Zhang S, Wang H, et al. An experimental research on regulatory effect of traditional Chinese medicine emodin on expression of aquaporin 3 in small intestine in rats with severe acute pancreatitis. *Chin J Integr Tradit West Med Intensive Crit Care (China)*. 2010;17:214–217.
35. Zhao YQ, Liu XH, Ito T, et al. Protective effects of rhubarb on experimental severe acute pancreatitis. *World J Gastroenterol*. 2004;10: 1005–1009.
36. Feng Z, Fei J, Wenjian X, et al. Rhubarb attenuates the severity of acute necrotizing pancreatitis by inhibiting MAPKs in rats. *Immunotherapy*. 2012;4:1817–1821.
37. Lei R, Wang Q, Zhang Z. Implementation of associated guidelines for severe acute pancreatitis. *Chin J Pract Surg*. 2012;7:523–524.